SCIENCE CHINA
Chemistry

• ARTICLES •
• SPECIAL TOPIC • Formation Mechanism and Control Strategies of Haze in China

September 2015 Vol.58 No.9: 1377–1384
doi: 10.1007/s11426-015-5414-x

Role of ammonia in forming secondary aerosols from gasoline vehicle exhaust

Tengyu Liu[1,2], Xinming Wang[1*], Wei Deng[1,2], Yanli Zhang[1], Biwu Chu[3], Xiang Ding[1], Qihou Hu[1], Hong He[3] & Jiming Hao[4]

[1]*State Key Laboratory of Organic Geochemistry, Guangzhou Institute of Geochemistry, Chinese Academy of Sciences, Guangzhou 510640, China*
[2]*University of Chinese Academy of Sciences, Beijing 100049, China*
[3]*Research Center for Eco-Environmental Sciences, Chinese Academy of Sciences, Beijing 100085, China*
[4]*State Key Joint Laboratory of Environment Simulation and Pollution Control, School of Environment, Tsinghua University, Beijing 100084, China*

Received January 25, 2015; accepted February 12, 2015; published online May 6, 2015

Ammonia (NH_3) plays vital roles in new particle formation and atmospheric chemistry. Although previous studies have revealed that it also influences the formation of secondary organic aerosols (SOA) from ozonolysis of biogenic and anthropogenic volatile organic compounds (VOCs), the influence of NH_3 on particle formation from complex mixtures such as vehicle exhausts is still poorly understood. Here we directly introduced gasoline vehicles exhausts (GVE) into a smog chamber with NH_3 absorbed by denuders to examine the role of NH_3 in particle formation from GVE. We found that removing NH_3 from GVE would greatly suppress the formation and growth of particles. Adding NH_3 into the reactor after 3 h photo-oxidation of GVE, the particle number concentration and mass concentrations jumped explosively to much higher levels, indicating that the numbers and mass of particles might be enhanced when aged vehicle exhausts are transported to rural areas and mixed with NH_3-rich plumes. We also found that the presence of NH_3 had no significant influence on SOA formation from GVE. Very similar oxygen to carbon (O:C) and hydrogen to carbon (H:C) ratios resolved by aerosol mass spectrometer with and without NH_3 indicated that the presence of NH_3 also had no impact on the average carbon oxidation state of SOA from GVE.

ammonia, vehicle exhaust, secondary organic aerosols (SOA), smog chamber, fine particles, nitrogen oxides, volatile organic compounds

1 Introduction

Ammonia (NH_3), a ubiquitous gas, is the third abundant nitrogen-containing gas in the atmosphere [1]. Atmospheric NH_3 is mainly emitted from animal waste, biological processes in soils and ammonia-based chemical fertilizers, followed by biomass burning, and sewage treatment plants [2,3]. The gas-phase reactions between NH_3 and inorganic acids such as nitric and sulfuric acid can form ammonium nitrate and sulfate [4], which are important constituents of airborne fine particles or $PM_{2.5}$ [5]. In China's megacities, which are frequently hard-hit by severe haze due to $PM_{2.5}$ pollution in the recent decade [6,7], ammonium alone has contributed more than 5% of the $PM_{2.5}$ mass [8–12].

NH_3 can enhance the nucleation of sulfuric acid particles and thus influence new particle formation events [13,14]. In addition, recent smog chamber simulations indicate that NH_3 can enhance the secondary organic aerosol (SOA) formation from ozonolysis of biogenic precursors by reacting with organic acids [15,16], but reduce SOA formation from the styrene-ozone system [17]. However, the potential

*Corresponding author (email: wangxm@gig.ac.cn)

influence of NH_3 on SOA formation is still poorly understood, especially for complex chemical mixtures such as vehicle exhausts brimming with thousands of gaseous and particle-phase components [18]. SOA, which is ubiquitous in various atmospheric environments, respectively accounts for approximately 66% and 90% of the total OA in urban as well as urban downwind and rural sites in Northern Hemisphere mid-latitudes [19]. Current chemical transport models usually underestimate the level of OA mainly due to the unclear formation processes and sources of SOA [20]. A detailed investigation of the potential influence of NH_3 on SOA formation from vehicle exhaust is therefore necessary to better understand the formation pathways and sources of SOA.

In urban areas with high population densities, NH_3 is centralized and significantly emitted from sewage. Recent tunnel studies indicated that emissions from light-duty gasoline vehicles (LDGVs) are also an important source of NH_3 [21–25]. Nordin *et al*. [26] found that SOA formed from the exhaust of idling gasoline vehicles could be 1–2 orders of magnitude higher than POA. Gordon *et al*. [18] and Platt *et al*. [27] also observed an enhancement of SOA/POA from 1 to 15 during the aging of emissions from LDGVs. Significant nitrate and ammonium were observed to be formed synchronously with SOA during the photo-oxidation of LDGV exhaust [18,26]. However, the formation of secondary aerosols including SOA, nitrate, and ammonium from vehicle exhaust still remain uncertain when NH_3 is removed. Therefore, studying the role of NH_3 in forming secondary aerosols from vehicle exhaust might give a better understanding of the tropospheric chemistry in urban areas, as well as the aging of vehicle exhausts transported into NH_3-rich plumes emitted from livestock waste and fertilizers in rural areas.

Here we introduce exhaust from LDGVs directly into a smog chamber with a 30 m^3 Teflon reactor with NH_3 absorbed by denuders, to study the role of NH_3 in particle formation under photo-oxidation. The purpose is to understand the effects of NH_3 on secondary aerosol formation from LDGV exhaust, and to obtain valuable information for the future emission control of NH_3 and vehicle exhaust.

2 Methods

2.1 Vehicles and fuel

Two port fuel injected Euro 1 and Euro 4 LDGVs with model years of 2002 and 2011 were used in this study. More details of each vehicle are listed in Table 1. They were fueled with Grade 93# gasoline, which complies with the Euro III gasoline fuel standard. The gasoline compositions were described in our previous study [28].

Table 1 Detailed information on the two light-duty gasoline vehicles

ID	Emission standard class	Vehicle	Model year	Mileage (km)	Displacement (cm^3)	Power (kW)	Weight (kg)
I	Euro4	Golf	2011	25000	1598	77	1295
II	Euro1	Accord	2002	237984	2298	110	1423

2.2 Smog chamber experiments

Six photochemical experiments were conducted in the smog chamber in Guangzhou Institute of Geochemistry, Chinese Academy of Sciences (GIG-CAS). The GIG-CAS smog chamber has a 30 m^3 fluorinated ethylene propylene (FEP) reactor housed in a temperature-controlled room. Details of setup and facilities about the chamber are described elsewhere [29]. Prior to each experiment, the chamber was evacuated and filled with purified dry air at least 5 times, after which the reactor was flushed with purified dry air for at least 48 h until no residual hydrocarbons, O_3, NO_x, or particles were detected. In the present study, temperature and RH inside the reactor were respectively set to 25 °C and 50%.

Before the introduction of vehicle exhaust, the test vehicle was at idling for at least 30 min to warm up the three-way catalysts. Next, vehicle exhaust was directly introduced into the reactor by two oil-free pumps (Gast Manufacturing, Inc, USA). For comparison, ammonia in LDGV exhaust from experiments I-2, II-2, and II-3 (Table 2) was absorbed by denuders coated with a solution of phosphorous acid in 1:9 water and ethanol [30].

After the introduction of exhaust, additional NO was added to adjust the VOC/NO_x ratios to 2.0–5.0 (Table 2), which was within the range of 0.5–10 in gasoline vehicle exhaust and downwind urban areas [31]. There were experiment-to-experiment differences in initial precursor concentrations due to the technical challenges of introducing the same amounts of exhaust into the reactor. We kept similar non methane hydrocarbons (NMHCs) concentrations for comparison experiments such as I-1 and I-2. After more than 30 min of primary characterization, the exhaust was continuously exposed to black light for 5 h. After the black lamps were switched off, the formed particles were characterized for another 2–3 h to correct the particle wall loss.

A series of instruments was used to characterize the gas- and particle-phase compounds in the reactor. Gas-phase ozone (O_3) and NO_x were measured online with dedicated monitors (EC9810 and 9841T, Ecotech, Australia). Methane and CO concentrations were determined using a gas chromatography (Agilent 6980GC, USA) with a flame ionization detector and a packed column (5A Molecular Sieve 60/80 mesh, 3 m×1/8 inch) [32], and CO_2 was analyzed with a gas chromatography (HP 4890D, USA) [33]. Gas-phase organic species such as C_6–C_{10} single-ring aromatic hydrocarbons were measured with a Mode 7100 preconcentrator (Entech Instruments Inc., USA) coupled with an

Table 2 Summary of the initial conditions and results of the light-duty gasoline vehicle photo-oxidation experiments

Exp # [a]	OH ($\times10^6$ molecules/cm^3)	T (°C)	RH (%)	VOC/NO_x	NMHCs (ppbv)	NO (ppbv)	NO_2 (ppbv)	SO_2 (ppbv)
I-1	1.20	24.2	52.5	2.0	1885	794.1	161.9	7.2
I-2 [b]	1.18	24.8	54.3	3.6	1821	496.9	2.8	6.8
II-1	0.80	24.6	55.6	3.0	5693	1833.3	45.9	14.7
II-2 [b]	0.79	24.4	54.6	3.9	4605	1117.8	63.3	15.0
II-3 [b]	0.84	25.1	51.9	4.4	1352	298.1	9.7	12.1
II-4 [c]	1.59	25.3	51.1	4.3	1303	296.2	4.4	13.3

a) Photooxidation experiments for exhausts from vehicles I and II, described in Table 1; b) for experiments I-2, II-2, and II-3, ammonia in LDGV exhaust was absorbed by denuders coated with a solution of phosphorous acid in 1:9 water and ethanol [30]. Around 100 ppb of NH_3 was injected after 4 h (experiment I-2) and 3 h of irradiation (experiment II-2); c) around 100 ppb of NH_3 was injected before UV irradiation.

Agilent 5973N gas chromatography-mass selective detector/ flame ionization detector/electron capture detector (GC-MSD/FID/ECD, Agilent Technologies, USA) [28,32,34,35] and a commercial proton-transfer-reaction time-of-flight mass spectrometer (PTR-TOF-MS, Model 2000, Ionicon Analytik GmbH, Austria) [36,37]. In this study, the decay curve of toluene measured by PTR-TOF-MS was used to derive the average hydroxyl radical (OH) concentration during each experiment.

Particle number concentrations and size distributions were measured with a scanning mobility particle sizer (SMPS, TSI Incorporated, USA; classifier model 3080, CPC model 3775). An aerosol density of 1.4 g cm^{-3} was assumed to convert the particle volume concentration into the mass concentration [38]. A high-resolution time-of-flight aerosol mass spectrometer (HR-TOF-MS, Aerodyne Research Incorporated, USA) was used to measure the particle chemical compositions and nonrefractory PM mass [39,40]. The instrument was operated in the high sensitivity V-mode and high resolution W-mode alternatively every two minutes. The toolkit Squirrel 1.51H was used to obtain the time series of various mass components (sulfate, nitrate, ammonium, and organics). We used the toolkit Pika 1.1H to determine the average element ratios of organics, like H:C, O:C, and N:C [41,42]. The contribution of gas-phase CO_2 to the *m*/*z* 44 signal was corrected using the measured CO_2 concentrations. The HR-TOF-MS was calibrated using 300 nm monodisperse ammonium nitrate particles.

2.3 Wall loss corrections

The loss of particles and organic vapors to the reactor walls must be accounted for to accurately quantify the SOA formation. Briefly, the loss of particles onto the walls has been well constrained and is treated as a first-order process [43]. The wall-loss rate constant was determined separately for each experiment by fitting the SMPS and AMS data when no new particles were formed. By applying this rate to the entire experiment, we used the same method as Pathak *et al*. [44] to correct the wall loss of the particles. In addition, the aerosol mass measured by HR-TOF-AMS was corrected with SMPS data with the same method used by Gordon *et al*. [18].

3 Results and discussion

3.1 Effects of NH_3 on particle formation and growth

To investigate the role of NH_3 in the formation of secondary aerosols from GVE, we conducted two experiments for each vehicle, with and without NH_3 absorbed by denuders. The detailed experimental conditions are listed in Table 2. The average concentration of OH radicals during the 5 h of irradiation was similar for each vehicle. Figure 1 shows the temporal evolution of gas-phase species, including NO, NO_2, and O_3, and the particle number concentrations during the photochemical aging experiments of LDGV exhaust with vehicle II. Between −2.1 and −1.5 h, the vehicle exhaust was introduced into the reactor, leading to a slight increase of the particle numbers before irradiation. In experiment II-2, NH_3 in the exhaust was absorbed by denuders. Obviously, in both experiments, NO was converted to NO_2 after the black lights were turned on. As presented in previous studies, a delay between aerosol formation and the start of irradiation is frequently observed in classic photo-oxidation experiments; specifically, aerosols may not form until the concentration of NO is around zero [45–47]. In the presence of NH_3, the number concentration of particles increased from ~1000 to ~4000 cm^{-3} when the concentration of NO was still hundreds of ppb (Figure 1(a)); without NH_3, no new particles were formed even when the concentration of NO was approximately zero (Figure 1(b)). Ng *et al*. [48] found that products formed under high NO conditions via RO_2+NO reactions partition much less readily into the aerosol phase than products formed via RO_2+HO_2 reactions under low NO conditions. Wildt *et al*. [47] observed that high concentration of NO was responsible for the suppression of new particle formation. Accordingly, higher concentration of NO in experiment II-1 than that in experiment II-2 should have suppressed new particle formation. However, new particle formation was observed only in experiment II-1, indicating that the presence of ammonia in LDGV exhaust might play an important role. Kirkby *et al*. [14] found that the presence of 100 ppt NH_3 could increase the nucleation rate of sulfuric acid particles by a factor of 100–1000. According to a recent study by Kulmala *et al*. [49], NH_3

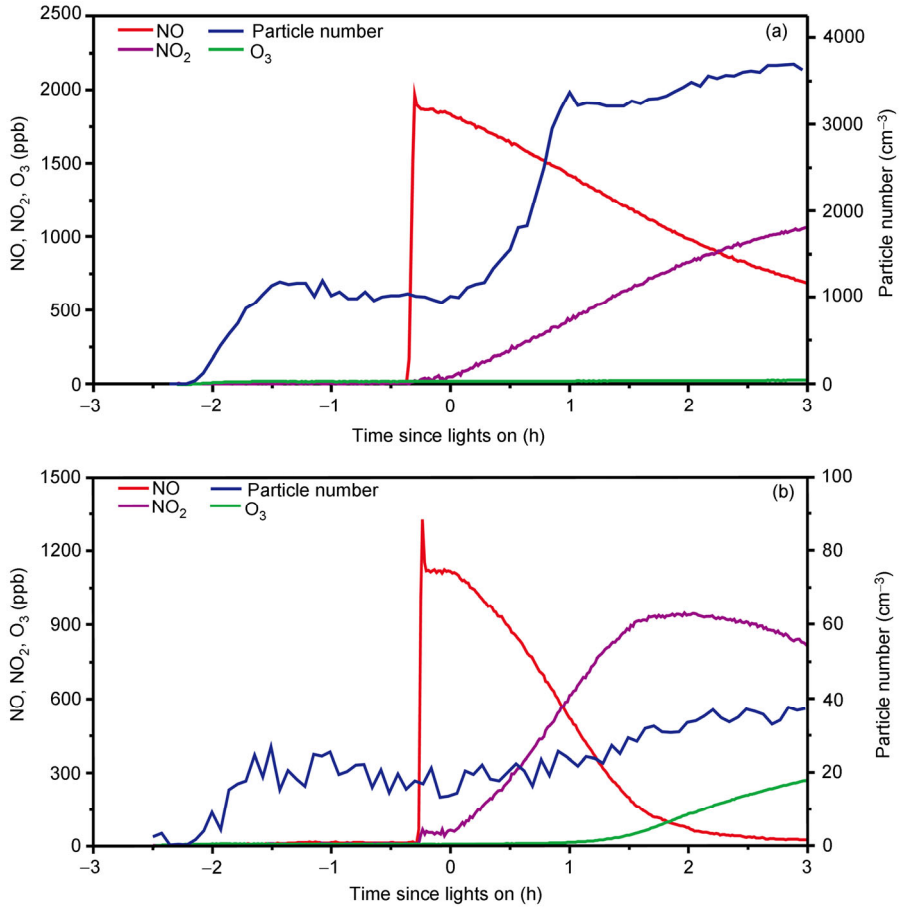

Figure 1 Concentration-time plots of gas-phase species and particle number concentrations in experiments II-1 (a) and II-2 (b) during 3 h of irradiation. The vehicle exhaust was introduced into the reactor between around −2.1 and −1.5 h; at time=0 h, the black lamps were turned on.

can stabilize initial sulfuric acid clusters with diameters of about 1.5 nm. These stable clusters are critical for new particle formation. As shown in Table 2, the initial concentration of SO_2 for vehicle II was around 15 ppb. NH_3 in GVE might stabilize sulfuric acid formed via the oxidation of SO_2 and thus facilitate new particle formation. Consequently, removing NH_3 in GVE suppressed new particle formation.

The geometric average diameter increased from 45 to 200 nm and from 22 to 220 nm in around 1 h for experiments I-1 and II-1, with respective particle growth rates of 139 and 181 nm h^{-1}; these rates were one order of magnitude higher than those observed in urban environments [50–52]. Some studies have shown that particles larger than 80 nm can be activated as cloud condensation nuclei (CCN) at moderate atmospheric supersaturation and that they possibly directly and indirectly impact climate [53,54]. Therefore, large amounts of LDGV exhaust emissions in urban areas via photochemical aging can influence air quality and even the climate.

As shown in Figure 2, a significant amount of ammonium nitrate was formed through the reaction of NH_3 with HNO_3 oxidized from NO in experiments I-1 and II-1. The maximum ammonium nitrate production was almost 7 times higher than SOA production, which indicated the significant contribution of LDGV exhaust to secondary inorganic aerosols. Nordin *et al.* [26] and Gordon *et al.* [18] also observed significant formation of ammonium nitrate during the aging of gasoline vehicle exhaust in smog chambers; in addition, in-use vehicle emissions mainly from LDGVs in a highway tunnel in Pittsburgh were also found to produce substantial ammonium nitrate [55]. Ammonium has frequently been observed to contribute to particle growth in urban environments [56–58]. Zhu *et al.* [52] hypothesized that ammonium nitrate plays a role in the particle growth in Qingdao and Toronto during spring. In Figure 3, we plot the concentration of ammonium nitrate without wall loss correction against the geometric average diameter derived from the SMPS data in experiments I-1 and II-1. In both experiments, the geometric average diameter showed significant linear correlations (R^2>0.84, P<0.001) with the concentration of ammonium nitrate, which demonstrated that ammonium nitrate plays an important role in the rapid growth of particles formed from the aging of LDGV exhaust.

A recent study indicated that the NH_3 emission factor of LDGVs in China was much higher than those in the United States [23]. However, today's emission standards for LDGV

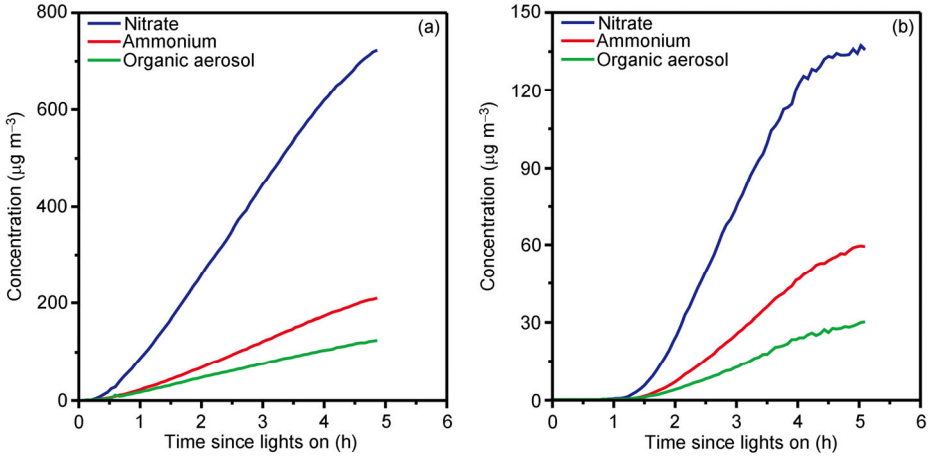

Figure 2 Concentration-time plots of nitrate, ammonium and organic aerosols in experiments. (a) I-1; (b) II-1.

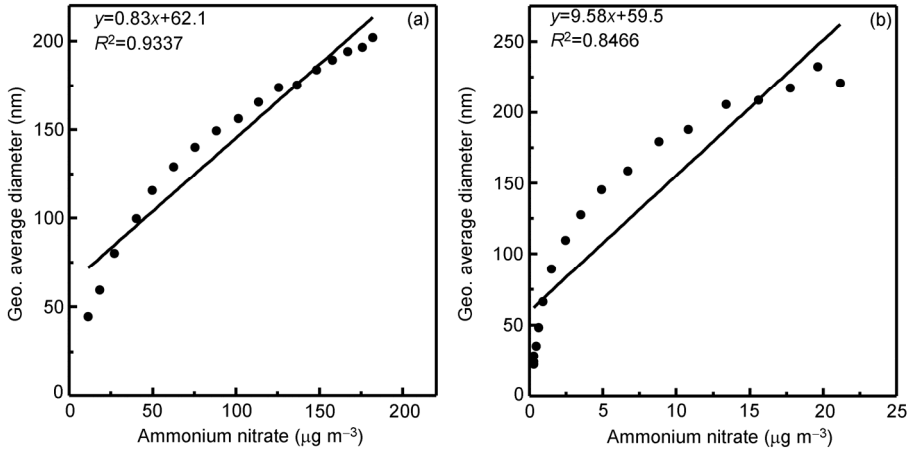

Figure 3 Scatter plots of geometric average diameter against the concentration of ammonium nitrate (without wall loss correction) in experiments I-1 (a) and II-1 (b). Plotted data of the concentration of ammonium nitrate were from around zero to the maximum.

exhaust concern only the primary emissions of hydrocarbon, NO_x, and CO. As the presence of NH_3 strongly enhances the formation and growth of particles from GVE, removing NH_3 from GVE might reduce secondary aerosols formation and benefit air pollution control in urban areas.

3.2 Effects of NH_3 on SOA formation

To further investigate the effects of NH_3 on SOA formation from LDGV exhaust, we conducted two more experiments, II-3 and II-4, with similar initial concentrations of VOCs and NO_x (Table 2). NH_3 in LDGV exhaust in experiment II-3 was absorbed by denuders, whereas in experiment II-4 around 100 ppb of NH_3 was injected before the UV lights were turned on. Variations of the geometric average diameters and concentrations of organic aerosols during the irradiation of LDGV exhaust with and without NH_3 are shown in Figure 4. With and without adding NH_3, the geometric average diameter respectively increased from around 20 nm to a maximum of 130 and 115 nm (Figure 4(a)). This result further demonstrates that the presence of NH_3 can enhance the growth of particles formed from the aging of LDGV exhaust. As shown in Figure 4(b), in the presence of NH_3, SOA was formed more slowly and its concentration was relatively lower. Because the average concentration of OH radicals during the whole experiment in the presence of NH_3 was higher, according to the gas-particle partitioning model [59], SOA formation under a higher OH concentration and similar concentrations of SOA precursors should be higher. Na *et al.* [15] observed that NH_3 could neutralize organic acids to enhance SOA formation from α-pinene ozonolysis. A recent study [60] demonstrated that NH_3 could react with carbonyl groups in SOA molecules to form nitrate-containing compounds. However, in our study the relatively lower concentration of SOA in the presence of NH_3 suggested that NH_3 might have no significant influences on SOA formation from LDGV exhausts.

The average oxygen to carbon (O:C) and hydrogen to carbon (H:C) molar ratios of SOA in experiments II-3 and II-4 are presented in Table 3. The O:C and H:C ratios in the

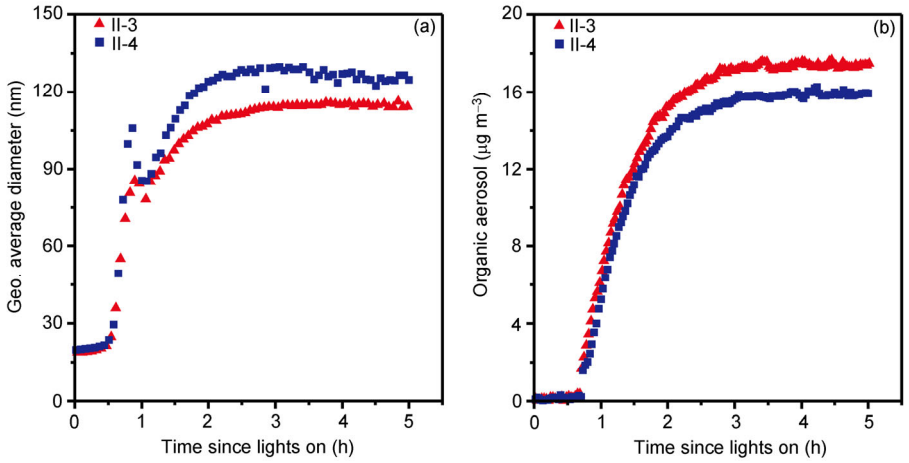

Figure 4 Geometric average diameter (a) and concentration of organic aerosols (b) in experiments II-3 (without NH_3) and II-4 (with NH_3).

presence of NH_3 were 0.683±0.042 and 1.352±0.042, respectively, almost same as the values without NH_3, indicating that the presence of NH_3 had no influence on the O:C and H:C ratios of SOA from LDGV exhaust. An average carbon oxidation state (OS_c) can be estimated from the O:C and H:C data [61]. The average OS_c of SOA formed from LDGV exhaust with and without NH_3 was 0.013 and 0.016, respectively, which are within or near the range of semi-volatile oxygenated OA (SV-OOA) (–0.5–0) [61] and are consistent with the observation of Nordin *et al.* [26]. The presence of NH_3 had no impact on the average OS_c of SOA from LDGV exhaust.

3.3 NH_3 with aged gasoline vehicle exhaust

With tremendous nitrogen fertilizer applications and animal feeding, in 2000 China contributed more than 55% of the NH_3 emissions in Asia [62]; in 2006, livestock waste and fertilizer in rural areas accounted for more than 85% of China's NH_3 emissions [63]. Obviously, mixing of NH_3 with aged GVE transported from urban areas is of concern for the air quality in rural areas. In the present study we added about 100 ppb of NH_3 into the reactor after 4 h (experiments I-2) and 3 h of irradiation (experiment II-2) to investigate the aerosol formation from aged GVE mixed with NH_3. Due to the unavailability of AMS data, herein we discuss only the influence of added NH_3 on the number and volume concentrations of particles. When NH_3 was added, the number and volume concentrations jumped immediately to higher levels (Figure 5). For experiment II-2, the number and volume concentrations of particles increased extremely fast to about 1×10^5 cm^{-3} and 40 μm cm^{-3}, respectively (Figure 5(a)). The addition of high concentrations of NH_3 might stabilize sulfuric acid clusters to overcome the nucleation barrier and thereby induce the burst particle formation [49]. If so, this would indicate that the numbers and mass of particles might be greatly enhanced when aged GVE is transported to rural areas and mixed with the substantial amounts of NH_3 emitted from livestock wastes and fertilizers. Reducing NH_3 emissions in the agricultural sector would therefore help lower both the number and mass contribu-

Table 3 Oxygen to carbon (O:C) ratio, hydrogen to carbon (H:C) ratio, and average carbon oxidation state (OS_c) in experiments II-3 and II-4

	O:C	H:C	OS_c
II-3	0.684±0.042	1.352±0.041	0.016
II-4	0.683±0.042	1.353±0.042	0.013

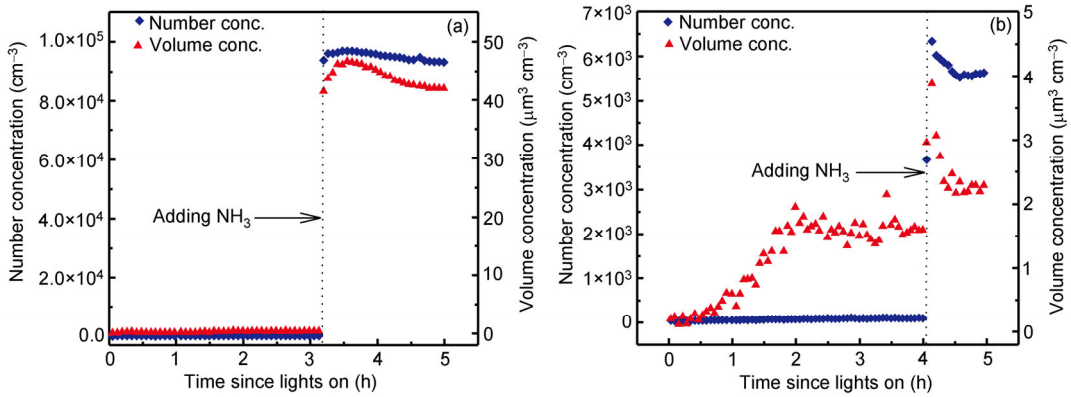

Figure 5 Effects of NH_3 on the formation of particles from aging LDGV exhaust in (a) II-2 and (b) I-2.

tions of fine particles in suburban and rural areas.

4 Conclusions

Smog chamber simulations about the formation of secondary aerosols from GVE with and without NH_3 absorbed by denuders revealed that the presence of NH_3 in GVE could enhance the formation and growth of particles. This indicates that control of NH_3 emissions in urban areas, as well as control of NH_3 in GVE, would suppress particle formation and growth during the early atmospheric evolution of GVE. Chamber simulations also revealed that particle numbers and mass concentrations increased rapidly to much higher levels when aged GVE was mixed with NH_3, suggesting that NH_3 from livestock waste and fertilizer applications would promote particle formation and growth when aged urban plumes reach rural areas. The present study therefore indicates NH_3 plays vital roles in particle growth and formation in both urban and rural areas. We also found that NH_3 had no significant effects on SOA formation from GVE or on the oxidation state of SOA.

This study was supported by the Strategic Priority Research Program of the Chinese Academy of Sciences (XDB05010200), the National Natural Science Foundation of China (41025012/41121063), NSFC-Guangdong Joint Funds (U0833003), and the Guangzhou Institute of Geochemistry (GIGCAS 135 Project Y234161001).

1 Seinfeld J, Pandis SN. *From Air Pollution to Climate Change, Atmospheric Chemistry and Physics*. 2nd ed. New York: John Wiley & Sons, 1998. 74–75
2 Bouwman AF, Lee DS, Asman WAH, Dentener FJ, Van Der Hoek KW, Olivier JGJ. A global high-resolution emission inventory for ammonia. *Glob Biogeochem Cycle*, 1997, 11: 561–587
3 Asman WAH. Factors influencing local dry deposition of gases with special reference to ammonia. *Atmos Environ*, 1998, 32: 415–421
4 Pinder RW, Adams PJ, Pandis SN. Ammonia emission controls as a cost-effective strategy for reducing atmospheric particulate matter in the eastern united states. *Environ Sci Technol*, 2007, 41: 380–386
5 Chow JC, Watson JG, Fujita EM, Lu Z, Lawson DR, Ashbaugh LL. Temporal and spatial variations of $PM_{2.5}$ and PM_{10} aerosol in the southern California air quality study. *Atmos Environ*, 1994, 28: 2061–2080
6 Chan CK, Yao X. Air pollution in mega cities in China. *Atmos Environ*, 2008, 42: 1–42
7 Zhang Q, He K, Huo H. Policy: cleaning China's air. *Nature*, 2012, 484: 161–162
8 He K, Yang F, Ma Y, Zhang Q, Yao X, Chan CK, Cadle S, Chan T, Mulawa P. The characteristics of $PM_{2.5}$ in Beijing, China. *Atmos Environ*, 2001, 35: 4959–4970
9 Pathak RK, Wu WS, Wang T. Summertime $PM_{2.5}$ ionic species in four major cities of China: nitrate formation in an ammonia-deficient atmosphere. *Atmos Chem Phys*, 2009, 9: 1711–1722
10 Yang F, Tan J, Zhao Q, Du Z, He K, Ma Y, Duan F, Chen G, Zhao Q. Characteristics of $PM_{2.5}$ speciation in representative megacities and across China. *Atmos Chem Phys*, 2011, 11: 5207–5219
11 Wang XM, Ding X, Fu XX, He QF, Wang SY, Bernard F, Zhao XY, Wu D. Aerosol scattering coefficients and major chemical compositions of fine particles observed at a rural site hit the central Pearl River Delta, South China. *J Environ Sci-China*, 2012, 24: 72–77
12 Fu XX, Wang XM, Guo H, Cheung K, Ding X, Zhao XY, He QF, Gao B, Zhang Z, Liu TY, Zhang YL. Trends of ambient fine particles and major chemical components in the Pearl River Delta region: observation at a regional background site in fall and winter. *Sci Total Environ*, 2014, 497–498: 274–281
13 Ortega IK, Kurtén T, Vehkamäki H, Kulmala M. The role of ammonia in sulfuric acid ion induced nucleation. *Atmos Chem Phys*, 2008, 8: 2859–2867
14 Kirkby J, Curtius J, Almeida J, Dunne E, Duplissy J, Ehrhart S, Franchin A, Gagné S, Ickes L, Kürten A, Kupc A, Metzger A, Riccobono F, Rondo L, Schobesberger S, Tsagkogeorgas G, Wimmer D, Amorim A, Bianchi F, Breitenlechner M, David A, Dommen J, Downard A, Ehn M, Flagan RC. Role of sulphuric acid, ammonia and galactic cosmic rays in atmospheric aerosol nucleation. *Nature*, 2011, 476: 429–433
15 Na K, Song C, Switzer C, Cocker DR. Effect of ammonia on secondary organic aerosol formation from α-pinene ozonolysis in dry and humid conditions. *Environ Sci Technol*, 2007, 41: 6096–6102
16 Huang Y, Lee SC, Ho KF, Ho SSH, Cao NY, Cheng Y, Gao Y. Effect of ammonia on ozone-initiated formation of indoor secondary products with emissions from cleaning products. *Atmos Environ*, 2012, 59: 224–231
17 Na K, Song C, Cocker Iii DR. Formation of secondary organic aerosol from the reaction of styrene with ozone in the presence and absence of ammonia and water. *Atmos Environ*, 2006, 40: 1889–1900
18 Gordon TD, Presto AA, May AA, Nguyen NT, Lipsky EM, Donahue NM, Gutierrez A, Zhang M, Maddox C, Rieger P, Chattopadhyay S, Maldonado H, Maricq MM, Robinson AL. Secondary organic aerosol formation exceeds primary particulate matter emissions for light-duty gasoline vehicles. *Atmos Chem Phys*, 2014, 14: 4661–4678
19 Zhang Q, Jimenez JL, Canagaratna MR, Allan JD, Coe H, Ulbrich I, Alfarra MR, Takami A, Middlebrook AM, Sun YL, Dzepina K, Dunlea E, Docherty K, DeCarlo PF, Salcedo D, Onasch T, Jayne JT, Miyoshi T, Shimono A, Hatakeyama S, Takegawa N, Kondo Y, Schneider J, Drewnick F, Borrmann S, Weimer S, Demerjian K, Williams P, Bower K, Bahreini R, Cottrell L, Griffin RJ, Rautiainen J, Sun JR, Zhang YM, Worsnop DR. Ubiquity and dominance of oxygenated species in organic aerosols in anthropogenically-influenced Northern Hemisphere midlatitudes. *Geophys Res Lett*, 2007, 34: L13801
20 Heald CL, Jacob DJ, Park RJ, Russell LM, Huebert BJ, Seinfeld JH, Liao H, Weber RJ. A large organic aerosol source in the free troposphere missing from current models. *Geophys Res Lett*, 2005, 32: L18809
21 Fraser MP, Cass GR. Detection of excess ammonia emissions from in-use vehicles and the implications for fine particle control. *Environ Sci Technol*, 1998, 32: 1053–1057
22 Durbin TD, Wilson RD, Norbeck JM, Miller JW, Huai T, Rhee SH. Estimates of the emission rates of ammonia from light-duty vehicles using standard chassis dynamometer test cycles. *Atmos Environ*, 2002, 36: 1475–1482
23 Burgard DA, Bishop GA, Stedman DH. Remote sensing of ammonia and sulfur dioxide from on-road light duty vehicles. *Environ Sci Technol*, 2006, 40: 7018–7022
24 Kean AJ, Littlejohn D, Ban-Weiss GA, Harley RA, Kirchstetter TW, Lunden MM. Trends in on-road vehicle emissions of ammonia. *Atmos Environ*, 2009, 43: 1565–1570
25 Liu TY, Wang XM, Wang BG, Ding X, Deng W, LV SJ, Zhang YL. Emission factor of ammonia (NH_3) from on-road vehicles in china: tunnel tests in urban Guangzhou. *Environ Res Lett*, 2014, 9: 064027
26 Nordin EZ, Eriksson AC, Roldin P, Nilsson PT, Carlsson JE, Kajos MK, Hellen H, Wittbom C, Rissler J, Londahl J, Swietlicki E, Svenningsson B, Bohgard M, Kulmala M, Hallquist M, Pagels JH. Secondary organic aerosol formation from idling gasoline passenger vehicle emissions investigated in a smog chamber. *Atmos Chem Phys*, 2013, 13: 6101–6116
27 Platt SM, El Haddad I, Zardini AA, Clairotte M, Astorga C, Wolf R, Slowik JG, Temime-Roussel B, Marchand N, Jezek I, Drinovec L, Mocnik G, Mohler O, Richter R, Barmet P, Bianchi F, Baltensperger U, Prevot ASH. Secondary organic aerosol formation from gasoline vehicle emissions in a new mobile environmental reaction chamber. *Atmos Chem Phys*, 2013, 13: 9141–9158
28 Zhang Y, Wang X, Zhang Z, LV S, Shao M, Lee FSC, Yu JZ. Species profiles and normalized reactivity of volatile organic compounds

from gasoline evaporation in China. *Atmos Environ*, 2013, 79: 110–118
29 Wang X, Liu T, Bernard F, Ding X, Wen S, Zhang Y, Zhang Z, He Q, Lv S, Chen J, Saunders S, Yu J. Design and characterization of a smog chamber for studying gas-phase chemical mechanisms and aerosol formation. *Atmos Meas Tech*, 2014, 7: 301–313
30 Perrino C, Gherardi M. Optimization of the coating layer for the measurement of ammonia by diffusion denuders. *Atmos Environ*, 1999, 33: 4579–4587
31 Clairotte M, Adam TW, Zardini AA, Manfredi U, Martini G, Krasenbrink A, Vicet A, Tournié E, Astorga C. Effects of low temperature on the cold start gaseous emissions from light duty vehicles fuelled by ethanol-blended gasoline. *Appl Energ*, 2013, 102: 44–54
32 Zhang Y, Wang X, Blake DR, Li LF, Zhang Z, Wang SY, Guo H, Lee FSC, Gao B, Chan L, Wu D, Rowland FS. Aromatic hydrocarbons as ozone precursors before and after outbreak of the 2008 financial crisis in the Pearl River Delta region, South China. *J Geophys Res*, 2012, 117: D15306
33 Yi Z, Wang X, Sheng G, Zhang D, Zhou G, Fu J. Soil uptake of carbonyl sulfide in subtropical forests with different successional stages in South China. *J Geophys Res*, 2007, 112: D08302
34 Wang X, Wu T. Release of isoprene and monoterpenes during the aerobic decomposition of orange wastes from laboratory incubation experiments. *Environ Sci Technol*, 2008, 42: 3265–3270
35 Zhang YL, Guo H, Wang XM, Simpson I, Barletta B, Blaked DR, Meinardi S. Emission patterns and spatiotemporal variations of halocarbons in the Pearl River Delta region, southern China. *J Geophys Res*, 2010, 115: D15309
36 Lindinger W, Hansel A, Jordan A. On-line monitoring of volatile organic compounds at pptv levels by means of proton-transfer-reaction mass spectrometry (PTR-MS) medical applications, food control and environmental research. *Int J Mass Spectrom Ion Process*, 1998, 173: 191–241
37 Jordan A, Haidacher S, Hanel G, Hartungen E, Märk L, Seehauser H, Schottkowsky R, Sulzer P, Märk TD. A high resolution and high sensitivity proton-transfer-reaction time-of-flight mass spectrometer (PTR-TOF-MS). *Int J Mass Spectrom*, 2009, 286: 122–128
38 Zhang Q, Worsnop DR, Canagaratna MR, Jimenez JL. Hydrocarbon-like and oxygenated organic aerosols in Pittsburgh: insights into sources and processes of organic aerosols. *Atmos Chem Phys*, 2005, 5: 3289–3311
39 Jayne JT, Leard DC, Zhang X, Davidovits P, Smith KA, Kolb CE, Worsnop DR. Development of an aerosol mass spectrometer for size and composition analysis of submicron particles. *Aerosol Sci Tech*, 2000, 33: 49–70
40 DeCarlo PF, Kimmel JR, Trimborn A, Northway MJ, Jayne JT, Aiken AC, Gonin M, Fuhrer K, Horvath T, Docherty KS, Worsnop DR, Jimenez JL. Field-deployable, high-resolution, time-of-flight aerosol mass spectrometer. *Anal Chem*, 2006, 78: 8281– 8289
41 Aiken AC, DeCarlo PF, Jimenez JL. Elemental analysis of organic species with electron ionization high-resolution mass spectrometry. *Anal Chem*, 2007, 79: 8350–8358
42 Aiken AC, DeCarlo PF, Kroll JH, Worsnop DR, Alex Huffman J, Docherty KS, Ulbrich IM, Mohr C, Kimmel JR, Sueper D, Sun Y, Zhang Q, Trimborn A, Northway M, Ziemann PJ, Canagaratna MR, Onasch TB, Rami Alfarra M, Prevot ASH, Dommen J, Duplissy J, Metzger A, Baltensperger U, Jimenez JL. O/C and OM/OC ratios of primary, secondary, and ambient organic aerosols with high-resolution time-of-flight aerosol mass spectrometry. *Environ Sci Technol*, 2008, 42: 4478–4485
43 McMurry PH, Grosjean D. Gas and aerosol wall losses in teflon film smog chambers. *Environ Sci Technol*, 1985, 19: 1176–1182
44 Pathak RK, Stanier CO, Donahue NM, Pandis SN. Ozonolysis of alpha- pinene at atmospherically relevant concentrations: temperature dependence of aerosol mass fractions (yields). *J Geophys Res-Atmos*, 2007, doi: 10.1029/2006JD007436
45 Hurley MD, Sokolov O, Wallington TJ, Takekawa H, Karasawa M, Klotz B, Barnes L, Becker KH. Organic aerosol formation during the atmospheric degradation of toluene. *Environ Sci Technol*, 2001, 35: 1358–1366
46 Johnson D, Jenkin ME, Wirtz K, Martin-Reviejo M. Simulating the formation of secondary organic aerosol from the photo-oxidation of toluene. *Environ Chem*, 2004, 1: 150–165
47 Wildt J, Mentel TF, Kiendler-Scharr A, Hoffmann T, Andres S, Ehn M, Kleist E, Müsgen P, Rohrer F, Rudich Y, Springer M, Tillmann R, Wahner A. Suppression of new particle formation from monoterpene oxidation by NO_x. *Atmos Chem Phys*, 2014, 14: 2789–2804
48 Ng NL, Kroll JH, Chan AWH, Chhabra PS, Flagan RC, Seinfeld JH. Secondary organic aerosol formation from *m*-xylene, toluene, and benzene. *Atmos Chem Phys*, 2007, 7: 3909–3922
49 Kulmala M, Kontkanen J, Junninen H, Lehtipalo K, Manninen HE, Nieminen T, Petäjä T, Sipilä M, Schobesberger S, Rantala P, Franchin A, Jokinen T, Järvinen E, Äijälä M, Kangasluoma J, Hakala J, Aalto PP, Paasonen P, Mikkilä J, Vanhanen J, Aalto J, Hakola H, Makkonen U, Ruuskanen T, Mauldin RL, Duplissy J, Vehkamäki H, Bäck J, Kortelainen A, Riipinen I, Kurtén T, Johnston MV, Smith JN, Ehn M, Mentel TF, Lehtinen KEJ, Laaksonen A, Kerminen VM, Worsnop DR. Direct observations of atmospheric aerosol nucleation. *Science*, 2013, 339: 943–946
50 Mönkkönen P, Koponen IK, Lehtinen KEJ, Hämeri K, Uma R, Kulmala M. Measurements in a highly polluted Asian mega city: observations of aerosol number size distribution, modal parameters and nucleation events. *Atmos Chem Phys*, 2005, 5: 57–66
51 Setyan A, Song C, Merkel M, Knighton WB, Onasch TB, Canagaratna MR, Worsnop DR, Wiedensohler A, Shilling JE, Zhang Q. Chemistry of new particle growth in mixed urban and biogenic emissions—insights from cares. *Atmos Chem Phys*, 2014, 14: 6477–6494
52 Zhu Y, Sabaliauskas K, Liu X, Meng H, Gao H, Jeong CH, Evans GJ, Yao X. Comparative analysis of new particle formation events in less and severely polluted urban atmosphere. *Atmos Environ*, 2014, 98: 655–664
53 Dusek U, Frank GP, Hildebrandt L, Curtius J, Schneider J, Walter S, Chand D, Drewnick F, Hings S, Jung D, Borrmann S, Andreae MO. Size matters more than chemistry for cloud-nucleating ability of aerosol particles. *Science*, 2006, 312: 1375–1378
54 Petters MD, Kreidenweis SM. A single parameter representation of hygroscopic growth and cloud condensation nucleus activity. *Atmos Chem Phys*, 2007, 7: 1961–1971
55 Tkacik DS, Lambe A, Jathar S, Li X, Presto AA, Zhao Y, Blake D, Meinardi S, Jayne JT, Croteau PL, Robinson AL. Secondary organic aerosol formation from in-use motor vehicle emissions using a potential aerosol mass reactor. *Environ Sci Technol*, 2014, 48: 11235–11242
56 Zhang Q, Stanier CO, Canagaratna MR, Jayne JT, Worsnop DR, Pandis SN, Jimenez JL. Insights into the chemistry of new particle formation and growth events in Pittsburgh based on aerosol mass spectrometry. *Environ Sci Technol*, 2004, 38: 4797–4809
57 Crilley LR, Jayaratne ER, Ayoko GA, Miljevic B, Ristovski Z, Morawska L. Observations on the formation, growth and chemical composition of aerosols in an urban environment. *Environ Sci Technol*, 2014, 48: 6588–6596
58 Zhang YM, Zhang XY, Sun JY, Lin WL, Gong SL, Shen XJ, Yang S. Characterization of new particle and secondary aerosol formation during summertime in Beijing, China. *Tellus B*, 2011, 63: 382
59 Pankow JF. An absorption-model of gas-particle partitioning of organic-compounds in the atmosphere. *Atmos Environ*, 1994, 28: 185–188
60 Updyke KM, Nguyen TB, Nizkorodov SA. Formation of brown carbon via reactions of ammonia with secondary organic aerosols from biogenic and anthropogenic precursors. *Atmos Environ*, 2012, 63: 22–31
61 Kroll JH, Donahue NM, Jimenez JL, Kessler SH, Canagaratna MR, Wilson KR, Altieri KE, Mazzoleni LR, Wozniak AS, Bluhm H, Mysak ER, Smith JD, Kolb CE, Worsnop DR. Carbon oxidation state as a metric for describing the chemistry of atmospheric organic aerosol. *Nat Chem*, 2011, 3: 133–139
62 Streets DG, Bond TC, Carmichael GR, Fernandes SD, Fu Q, He D, Klimont Z, Nelson SM, Tsai NY, Wang MQ, Woo JH, Yarber KF. An inventory of gaseous and primary aerosol emissions in Asia in the year 2000. *J Geophys Res*, 2003, 108: 8809
63 Huang X, Song Y, Li M, Huo Q, Cai X, Zhu T, Hu M, Zhang HS. A high-resolution ammonia emission inventory in China. *Glob Biogeochem Cycle*, 2012, doi: 1010.1029/2011GB004161